RESEARCH PAPER

3D laser metal deposition: process steps for additive manufacturing

B. Graf [1] · A. Marko [1] · T. Petrat [1] · A. Gumenyuk [1,2] · M. Rethmeier [1,2,3]

Abstract

Laser metal deposition (LMD) is an established technology for two-dimensional surface coatings. It offers high deposition rates, high material flexibility, and the possibility to deposit material on existing components. Due to these features, LMD has been increasingly applied for additive manufacturing of 3D structures in recent years. Compared to previous coating applications, additive manufacturing of 3D structures leads to new challenges regarding LMD process knowledge. In this paper, the process steps for LMD as additive manufacturing technology are described. The experiments are conducted using titanium alloy Ti-6Al-4V and Inconel 718. Only the LMD nozzle is used to create a shielding gas atmosphere. This ensures the high geometric flexibility needed for additive manufacturing, although issues with the restricted size and quality of the shielding gas atmosphere arise. In the first step, the influence of process parameters on the geometric dimensions of single weld beads is analyzed based on design of experiments. In the second step, a 3D build-up strategy for cylindrical specimen with high dimensional accuracy is described. Process parameters, travel paths, and cooling periods between layers are adjusted. Tensile tests show that mechanical properties in the as-deposited condition are close to wrought material. As practical example, the fir-tree root profile of a turbine blade is manufactured. The feasibility of LMD as additive technology is evaluated based on this component.

Keywords Laser metal deposition · Build-up strategy · Deposition rate · Additive manufacturing

1 Introduction

Today, the trend to individualized products and decreasing time to market leads to an industrial demand for flexible manufacturing technologies [1]. These technologies must allow the resource-efficient production of long-life capital goods. Additive manufacturing technologies offer high flexibility regarding complex design features and allow direct manufacturing from CAD data without tooling, therefore saving time and costs [2]. Additive processes gain an importance especially in the aviation industry, where components with

high "buy-to-fly" ratio are common. For example, the machining of a blade integrated disk from forgings leads to a material loss of around 80–90%. In these cases, additive technologies have a high potential for material savings. A prominent laser-based method is laser metal deposition (LMD), which has been applied as coating technology for over 20 years. Additive manufacturing of 3D parts with LMD emerged as a new field of application. In order to apply LMD as additive technology, new process knowledge is necessary to adjust the weld bead size, to create a build-up strategy for high net shape, and to understand the achievable mechanical properties.

This article is part of the collection Welding, Additive Manufacturing and Associated NDT

✉ B. Graf
  benjamin.graf@ipk.fraunhofer.de

1 Fraunhofer IPK, Pascalstraße 8-9, 10587 Berlin, Germany

2 Bundesanstalt für Materialforschung und –prüfung BAM, Unter den Eichen 87, 12205 Berlin, Germany

3 Technische Universität Berlin, Straße des 17. Juni, 10623 Berlin, Germany

2 State of the art

LMD is shown in Fig. 1. The process utilizes a powder nozzle for material delivery. Powder particles are transported with a carrier gas, while the laser beam creates a molten pool on the substrate. After solidification, single weld beads are formed. In additive manufacturing, these weld beads are placed next to each other to form layers, and multiple layers on top of each other form volumes.
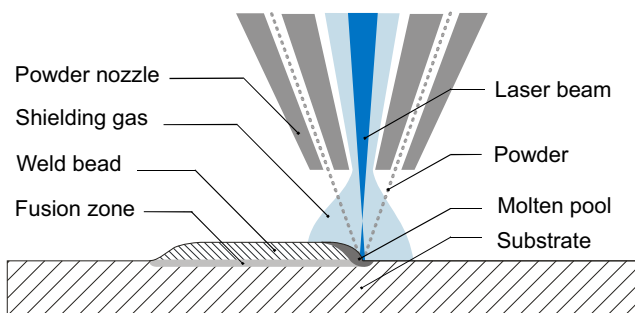
Fig. 1 Laser metal deposition process

Table 1 Chemical composition of Ti-6Al-4V powder material in weight %

Al	V	Fe	O	N	C	H	Ti
6.40	4.06	0.19	0.12	0.005	0.005	0.003	bal.

LMD as additive manufacturing technology for Ti-6Al-4V and Inconel 718 is described in [3]. Material deposition for repair purposes and resulting mechanical properties are shown in [4, 5].

Compared to previous coating applications, additive manufacturing of 3D structures brings new challenges regarding LMD process knowledge:

Knowledge about the influence of process parameters on weld bead geometry is necessary, to adjust the bead size for the component geometry. This knowledge can be obtained with well-designed experiments [6]. Additive manufactured parts consist of many superimposed layers. Irregularities in a single layer add up over multiple layers and can lead to geometrical deviations or low mechanical properties [7]. Level layer surfaces are necessary to prevent that. Areas with different deposition rates must be identified to control the error propagation. Hensinger et al. [8] studied a lower deposition rate in edge areas and made use of an inclined position of the powder nozzle. This requires enough space to prevent collisions with surrounding parts and a stable powder jet, which allows for nozzle inclination. Petrat et al. used different bead geometries to achieve a near-net shape deposition for the repair of a gas turbine burner [9].

A summary for additive manufacturing with LMD is given in [10]. A single layer can be deposited with
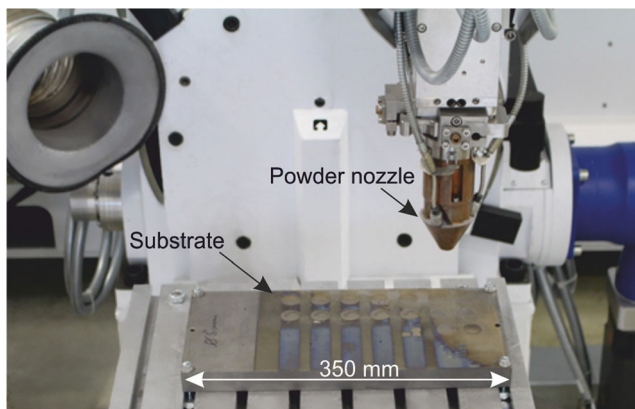

Fig. 2 Experimental setup

different travel paths. A common travel path is a contour track, followed by a pendulum strategy to fill the interior [11]. Welding of multiple layers on top of each other leads to heat accumulation. This increases the molten pool and changes the weld bead height and width. Furthermore, cooling times are prolonged. The build-up strategy must be adjusted to deal with these issues. For a stable build-up process, cooling periods between the single layers or adjustments of the laser power can be applied [12]. This is of high relevance for titanium alloys, since they are susceptible to reaction with atmospheric gases, which leads to embrittlement. A good shielding gas atmosphere is necessary. Combined with heat accumulation in additive manufacturing, and low heat dissipation in the additive build-up of 3D structures, this leads to challenging manufacturing. In the state of the art, three different approaches haven been outlined to deal with this issue:

- Additional nozzles for increased shielding gas atmosphere. Experiences with trailing nozzles exist from fusion welding. An additional ring nozzle is applied in [13] to cover deposited material in LMD build-up of a turbine blade. The main disadvantage of additional nozzles is a decreased geometrical flexibility.
- Process chamber, open or closed, flooded with argon as shielding gas. A constant flow of argon gas displaces atmospheric gases in the process chamber. A box of this kind was applied for LMD by Brandl [14]. The disadvantage of this solution is that the process chamber limits the specimen size. Furthermore, it impedes the movement and inclination of the powder nozzle, so it is difficult to adjust the build-up strategy.
- Deposition close to the substrate: The substrate plate provides good heat dissipation; therefore, the requirements for the shielding gas atmosphere are reduced. Tensile test specimens of this kind are manufactured by Yu et al. [15]. The disadvantage of this manufacturing version is that it is not a representative test for additive manufacturing with

Table 2 Full factorial experimental design for Ti-6Al-4V

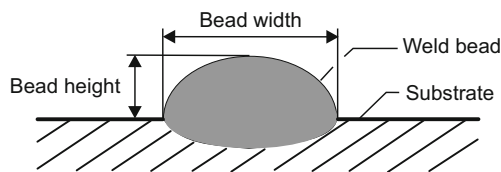| Factor steps	P in W	d in mm	v in mm/min	m in g/min
+ 1	1700	1.8	680	7.9
− 1	800	1.2	320	3.8

Fig. 3 LMD weld bead

LMD. Heat accumulation does not take place close to the substrate, whereas it increases in the additive build-up of 3D structures the higher the structure gets.

While the three described methods work well in their respective application, they are not able to fully comply with the demands of LMD as additive manufacturing technology. For an additive LMD process, a high geometrical flexibility for the powder nozzle is necessary to adjust build-up strategy and to deposit material on existing parts with complex shape. These demands are fulfilled if the shielding gas atmosphere is created only by a single LMD nozzle, although issues with the restricted size and quality of the local shielding gas atmosphere arise.

The aim of this paper is to discuss the necessary process knowledge for LMD as additive manufacturing technology.

3 Experimental

The metal deposition is conducted with a TRUMPF TruDisk Yb:Yag laser. Helium 5.0 is used as carrier gas for the powder material with 4 l/min, and argon 5.0 as shielding gas with 10 l/min. The 3-jet powder nozzle is positioned by a 5-axis machine.

The experiments are conducted with typical materials from turbine engines, namely titanium alloy Ti-6Al-4V and nickel-based alloy Inconel 718. The process knowledge about weld
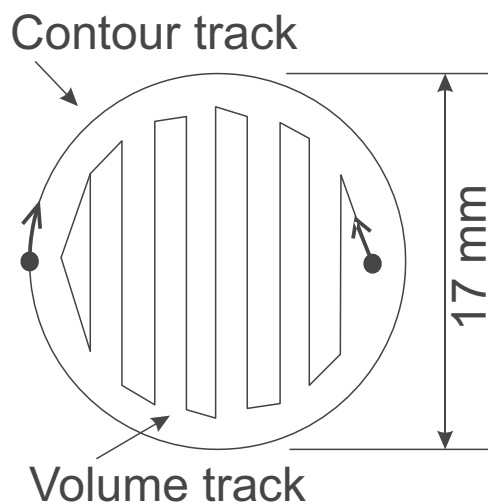
Table 3 Process parameters for cylindrical specimen, Ti-6Al-4V

P in W	d in mm	v in mm/min	m in g/min
1000	1.0	1000	3.8

bead geometry and build-up strategy is obtained for Ti-6Al-4V. In the next step, the build-up strategy for the complex geometrical shapes of a demonstrative turbine blade is designed. This blade is manufactured with Inconel 718.

3.1 Weld bead geometry

Ti-6Al-4V powder with a powder diameter range of 45–125 μm is deposited on a Ti-6Al-4V substrate plate. All edges of the plate are fixed to the table to avoid distortion during the build-up process. Figure 2 shows the experimental setup. The chemical composition of the powder is shown in Table 1.

For the deposition of single weld beads, the process parameter laser power P, laser spot diameter d, welding velocity v and powder mass flow m are varied with a full factorial experimental design according to Table 2. Each parameter combination is repeated three times.

Width and height of the weld bead dimension are measured (see Fig. 3). The results are evaluated with multiple regression based on a linear model, considering only significant effects.

3.2 LMD build-up strategy for cylindrical specimen

Cylindrical test specimens with a diameter of 17 mm and a height of 120 mm are manufactured with Ti-6Al-4V. The specimen consists of 240 single layers on top of each other.
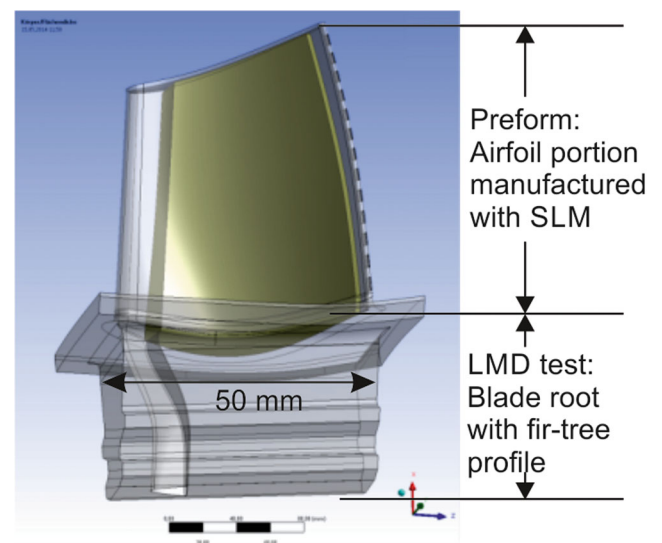

Fig. 4 Travel path for cylindrical specimen

Fig. 5 Demonstrative component, turbine blade

Table 4 Bead geometry in mm, Ti-6Al-4V, full factorial design

	Minimum	Mean	Maximum	Mean standard deviation
Width	2.2	3.3	4.7	0.07
Height	0.5	0.9	1.6	0.05

The following deposition strategy is applied: Along the contour, single weld beads are deposited with a circular nozzle path. For the inner volume, straight weld beads are placed next to each other. Figure 4 shows the nozzle path. The cladding direction is rotated in each layer. Five specimens are built at the same time. After the deposition process for one layer is finished, the shielding gas flow is kept active for an additional 10 s to provide shielding during the cooling process. The process parameters are shown in Table 3.

3.3 Tensile test

From the cylindrical specimens, five tensile test specimens are manufactured by turning. Dimensions are chosen according to DIN 50125 shape A with a diameter of 5 mm. Tensile tests are performed with a MTS 810 system and a test speed of 0.0333 mm/s.

3.4 Demonstrative component

A turbine blade is chosen as demonstrative example (see Fig. 5). First, the airfoil portion of the blade is manufactured with selective laser melting (SLM), an additive process using a powderbed. This airfoil portion serves as preform for the LMD practical example.

In the second step, additive manufacturing with LMD is applied to build the root of the blade with its fir-tree profile.

Table 5 Effects and interactions for weld bead geometry (linear model, multiple regression analysis, only significant effects)

|		Height		Width	
		Effect	p value	Effect	p value
Effects	P	0.04	0.036	1.35	0.000
	d	–	–	0.11	0.017
	v	− 0.48	0.000	− 0.84	0.000
	m	0.52	0.000	0.18	0.000
Interactions	Pd	–	–	− 0.12	0.011
	Pv	–	–	− 0.27	0.000
	Pm	–	–	− 0.14	0.002
	dv	–	–	–	–
	dm	–	–	–	–
	vm	− 0.17	0.000	–	–
Coefficient of determination R^2		0.98		0.97	
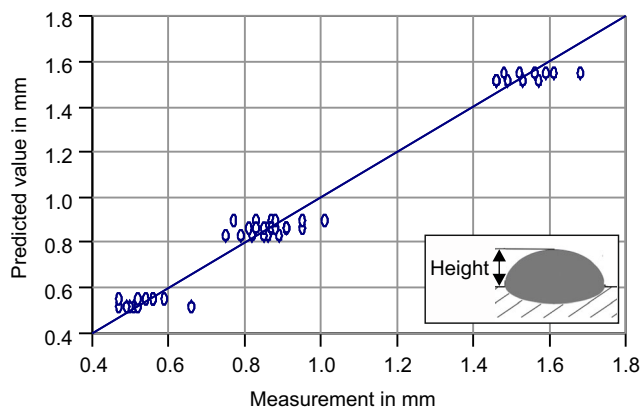
Fig. 6 Bead height, predicted values and measurement, linear model, Ti-6Al-4V

The root is manufactured with two different parameter sets. One parameter set is optimized for high accuracy, while the second set is chosen in order to build massive volumes with a low number of layers. Every five layers, cooling periods of 3 min were made to prevent heat accumulation. The blade is manufactured from nickel-based alloy Inconel 718.

4 Results and discussion

4.1 Weld bead geometry

Table 4 shows the measured bead geometry for the full factorial design. The difference in bead width between minimum and maximum is 2.5 mm; for the bead height, it is 1.1 mm. This is a substantial difference, which allows adjusting the bead shape in additive manufacturing for the specific component geometry. This difference also confirms that the parameter window chosen according to Table 2 is large enough for the demands of additive manufacturing with LMD. The standard deviation is determined for each parameter combination individually and given in Table 4 as mean value over all
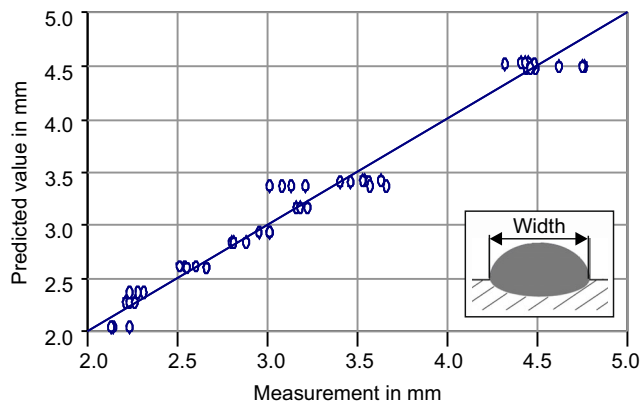
Fig. 7 Bead width, predicted values and measurement, linear model, Ti-6Al-4V

Fig. 8 Cylindrical specimen, 240 layers Ti-6Al-4V
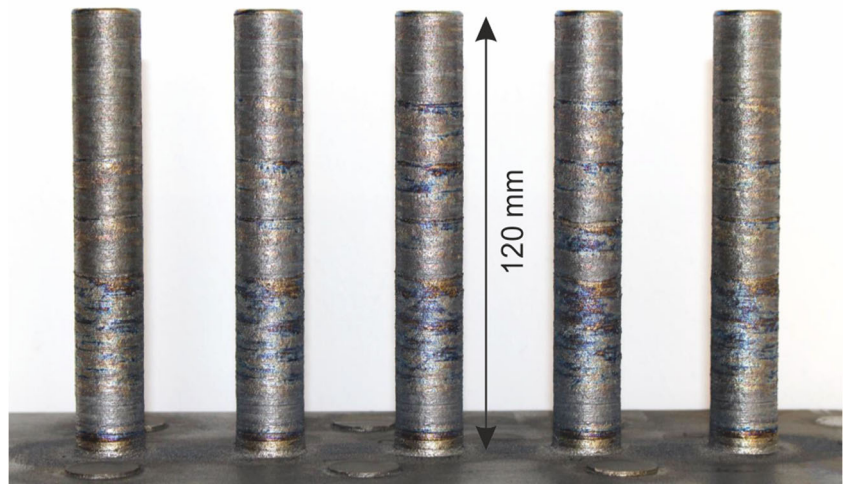
parameter combinations. The low mean standard deviation indicates a stable process with low variance in the bead geometry.

Table 5 shows the results of the regression analysis. The multiple regression removes effects and interactions which are not significant from the model. An effect is considered as significant if its p value is below 0.05. The model shows a coefficient of determination of 0.98 for bead height and 0.97 for bead width. Therefore, a good correlation of the model with the measured values is achieved.

Powder mass flow has the largest effect on bead height. During the deposition process, the powder is layered on the molten pool. As long as the process is stable with sufficient energy input, the powder material is included in the resulting weld bead. Due to the powder being layered on top of the existing material, rather than alongside of it, the bead height is affected. If too much powder is applied, the process is no longer able to melt all the particles. This leads to no adhesion and an unstable process.

Besides powder mass flow, the bead height is influenced by the welding velocity. A low velocity means more powder material is injected in the same welding distance, so additional material is available to form a high weld bead. Furthermore, a low welding velocity leads to an increased energy input per unit length, providing more energy to melt additional particles.

The bead width is strongly influenced by the laser power. A high laser power creates a large molten pool, which will lead to wider weld beads. The effect of the velocity can be explained in a similar way. A low velocity means a higher energy input, and therefore a larger molten pool.

Regarding the interactions in Table 5, it is interesting that the largest effect is contributed to the interaction of power P and velocity v (for bead width). Both parameters are quite commonly assessed together in joint welding as "energy input per unit length," which is power divided by velocity. For

deposition welding, the interaction of power and velocity proves that the energy input per unit length is also a useful calculation to assess a certain parameter combination.

A comparison of predicted values according to the model and the measurements is given in Figs. 6 and 7. The straight line represents the ideal case, in which the model predictions match the measurements. Due to measurement inaccuracy and random influence, this ideal case is not possible in real-world experiments.

All measurement values are quite close to the predicted values, which confirms the good correlation of the model. It is important to note that the size of the residuals is not dependent on the value of the measurement. This is a fulfilled requirement for the validity of the statistical analysis, and therefore, the interpretation of the statistical results is possible.
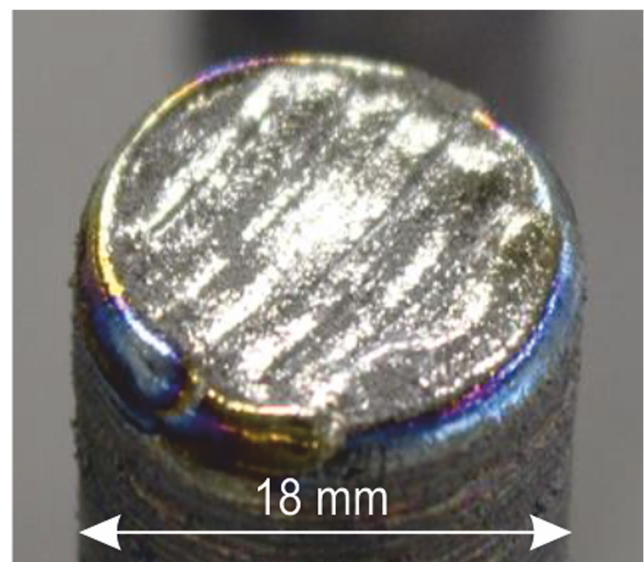
Fig. 9 Heat tint on specimen surface, Ti-6Al-4V

Table 6 Mechanical properties of Ti-6Al-4V specimen: own specimen and ASTM specification

Material condition	Yield strength in MPa	Tensile strength in MPa	Elongation in %
LMD specimen, as deposited	876 ± 6	923 ± 9	10.1 ± 1.5
Cast material ASTM F1108	> 758	> 860	> 8
Wrought material ASTM F1472	> 860	> 930	> 10

The values for bead height in Fig. 6 are grouped in three clusters. This behavior can be explained by the effects according to Table 5. The height is mainly determined by velocity and powder mass flow. In the full factorial design, both parameters are used with a high (+ 1) and a low (− 1) value, which leads to four combinations. The cluster with the highest value for bead height is created by high powder mass flow (+ 1) and low velocity (− 1). The opposite combination of low powder mass flow (− 1) and high velocity (+ 1) leads to the lower cluster. The middle cluster is created by the other two combinations. Due to the interaction of velocity and mass flow (see Table 5), the middle cluster is closer to the lower cluster.

For additive manufacturing applications of LMD, the knowledge about the effects on weld bead geometry is necessary to adjust the bead size for the component geometry. Large weld beads are beneficial for high deposition rates, while smaller weld beads allow better net shape deposition.

4.2 LMD build-up strategy for cylindrical specimen

Figures 8 and 9 show the manufactured specimen and the top surface. The inner surface is bright without heat tint, so good shielding gas coverage was achieved. Along the contour, golden and blue heat tint is visible which indicates reaction with atmospheric gases. The heat tint along the contour can be explained by lower heat deduction and shorter shielding gas coverage during the deposition of the circular contour track. The task of the contour track is to allow for a good net shape deposition process, while the inner volume needs to fulfill requirements for mechanical properties. In this case, heat tint along the contour can be accepted and the build-up strategy was not modified to avoid them. The tensile test specimens are manufactured from the center volume, which shows a bright surface.

Welding time ("laser on") for all five cylindrical specimens is around 6.8 h. In order to get the manufacturing time, 10 s after each layer has to be added for the continuous shielding gas flow after welding. For five cylinders comprising of 240 layers each, this amounts to 3.3 h. This indicates a limitation of a deposition process without an inert gas chamber. Depending on part volume, geometry, and batch size, additional manufacturing time has to be accepted in order to provide feasible shielding gas coverage during the cooling period. For larger batch sizes, the additional shielding gas flow time decreases, since a single specimen can cool down while the welding process is continued on the other specimens.

4.3 Tensile test

The tensile test results are shown in Table 6. Compared to the reference values of ASTM F1108 and ASTM F1472, it can be concluded that good mechanical properties are achieved. They are better than cast material specification and close to wrought material specification. The results show that it is possible to achieve good mechanical properties in the additive build-up of 3D specimen, despite heat accumulation and low heat dissipation, although prolonged manufacturing times for cooling periods have to be accepted.

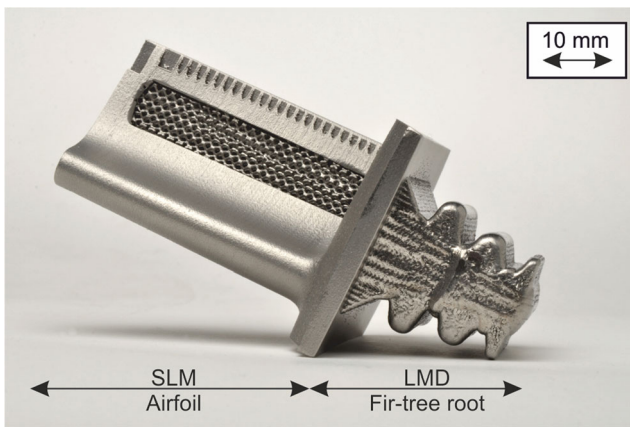**Fig. 10** Demonstrative example: preform (left) and LMD process (right)
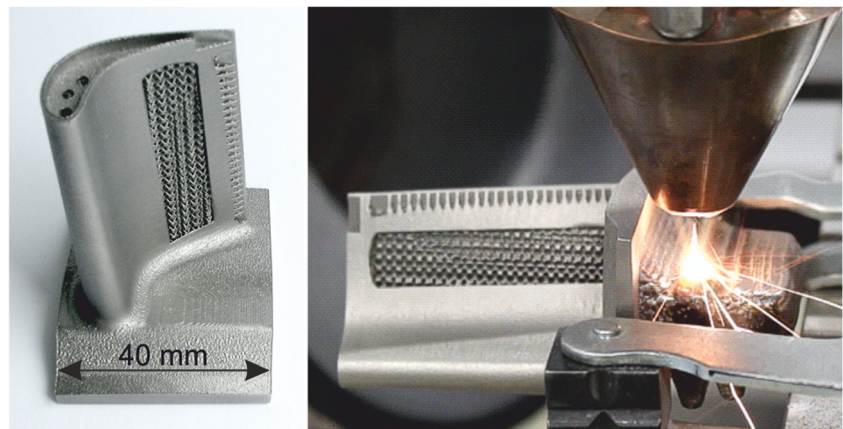
Fig. 11 Demonstrative example: LMD build-up of fir-tree root

4.4 Demonstrative example

The preform (airfoil portion of the blade) is shown in Fig. 10. The powderbed manufacturing with SLM allows the integration of lightweight grid structures in this component, which could be used to save weight while maintaining high stiffness. Figure 10 also displays the LMD process during the root manufacturing.

The final product comprising the fir-tree root produced with LMD is shown in Fig. 11. Since this is a high precision part, further machining via CNC milling is required independent of the production method with LMD only or more precise methods like powderbed-based additive technologies.

To avoid heat accumulation, the process knowledge about cooling periods obtained in the cylindrical specimen has to be applied. Since Inconel 718 is far less susceptible to reaction with atmospheric gases than titanium alloys, a cooling period of 3 min every five layers proves to be enough.

Necessary cooling periods limit the productivity and therefore the economic feasibility of LMD as additive technology. In order to increase it, multiple blades can be manufactured at the same time, using cooling periods on one blade for continued material deposition on the next blade. That way, the process is utilized most efficiently. For the exemplary fir-tree profile, a batch size of 18 blades allows for a continuous material deposition and leads to a welding time (laser on) of 36 min per blade.

5 Conclusion

Laser metal deposition as additive technology requires the adjustment of single weld bead geometries for the component shape. Therefore, this paper shows the effect of process parameters on bead geometry. Bead width is mainly determined by laser power, while the main effect on bead height is the welding velocity.

It is possible to manufacture specimen with high aspect ratio and local shielding gas atmosphere, even for alloys susceptible to embrittlement like Ti-6Al-4V. The manufacturing time has to be increased in order to allow a continued shielding gas flow after welding of each layer. Mechanical properties close to wrought material specification are achieved.

Shape complexity is not limited to simple cylindrical or cubic geometries. The fir-tree root of a turbine blade can be manufactured with LMD. Productivity increases with higher batch sizes, when cooling periods on one component are utilized for continued deposition on the next component.

References

1. Caffrey T, Wohlers T (2015) Wohlers report 2015: additive manufacturing and 3D printing state of the industry
2. Levy G, Schindel R, Kruth J-P (2003) Rapid manufacturing and rapid tooling with layer manufacturing (LM) technologies, state of the art and future perspectives. CIRP Ann – ManufTechnol 52(2)
3. Kool G, Amsterdam E (2010) Laser additive manufacturing of titan and inconel, future of gas turbine technology—5th International Conference, Brussels, Belgium
4. Graf B, Gumenyuk A, Rethmeier M (2012) Laser metal deposition as repair technology for stainless steel and titanium alloys. Phys Procedia 39:376–381
5. Korinko P, Adams T, Malene S (2011) Laser engineered net shaping for repair and hydrogen compatibility. Weld J 90:171–181
6. Graf B, Ammer S, Gumenyuk A, Rethmeier M (2013) Design of experiments for laser metal deposition in maintenance, repair and overhaul applications. Procedia CIRP 11:245–248
7. Petrat T, Graf B, Gumenyuk A, Rethmeier M (2015) Build-up strategies for generating components of cylindrical shape with laser metal deposition, Lasers in Manufacturing Conference 2015, München, Germany
8. Hensinger M, Ames A, Kuhlmann J (2000) Motion planning for a direct metal deposition rapid prototyping system, robotics and automation, proceedings. ICRA '00
9. Petrat T, Graf B, Gumenyuk A, Rethmeier M (2016) Laser metal deposition as repair technology for a gas turbine burner made of inconel 718. Phys Procedia 83:761–768
10. Costa L, Vilar R (2009) Laser powder deposition. Rapid Prototyp J 15(4):264–279
11. Rombouts M, Maes G, Hendrix W, Delarbre E, Motmans F (2013) Surface finish after laser metal deposition. Phys Procedia 41:810–814
12. Ocylok S, Alexeev E, Mann S, Weisheit A, Wissenbach K, Kelbassa I (2014) Correlations of melt pool geometry and process parameters during laser metal deposition by coaxial process monitoring. Phys Procedia 56:228–238
13. Gasser A, Witzel J, Goebel M (2013) Additive manufacturing of turbo-engines applications. ICTM conference, Aachen
14. Brandl E, Baufeld B, Leyens C, Gault R (2010) Additive manufactured Ti-6Al-4V using welding wire: comparison of laser and arc beam deposition and evaluation with respect to aerospace material specifications, LANE. Phys Procedia 5:595–606
15. Yu J, Rombouts M, Maes G, Motmans F (2012) Material properties of Ti6Al4V parts produced by laser metal deposition. Phys Procedia 39:416–424